

Enhancement of near-band-edge photoluminescence from ZnO films by face-to-face annealing

Y.G. Wang^a, S.P. Lau^{a,*}, X.H. Zhang^b, H.H. Hng^c, H.W. Lee^a, S.F. Yu^a,
B.K. Tay^a

^a *School of Electrical and Electronic Engineering, Nanyang Technological University, Block SI, Nanyang Avenue, Singapore 639798, Singapore*

^b *Institute of Materials Research and Engineering, Research Link, Singapore 117602, Singapore*

^c *School of Materials Engineering, Nanyang Technological University, Singapore 639798, Singapore*

Received 14 July 2003; accepted 31 July 2003

Communicated by D.P. Norton

Abstract

The influence of post-growth annealing on the luminescent properties of ZnO films was investigated. The non-radiative recombination centers in the films can be removed effectively by annealing at high temperature. Annealing in open ambient caused visible luminescence related defect centers to be formed and degraded the emission efficiency of near band edge (NBE) ultraviolet photoluminescence. To overcome this problem, a face-to-face annealing technique is used. It is found that by confining the surface of the films exposed to the ambient during annealing, the luminescent efficiency of NBE ultraviolet emission is enhanced significantly, and the formation of visible luminescence related defect centers is suppressed. This is attributed to the reduction in the rate of formation of vacancies (oxygen and/or zinc) at the surface region, which in turn decreases the bulk defect density in the ZnO films. The sublimation of ZnO is suppressed effectively by face-to-face annealing, and the roughness of the film surface is also improved, as compared to annealing in open air. © 2003 Elsevier B.V. All rights reserved.

PACS: 78.55.Et; 81.15.Ef; 81.05.Dz

Keywords: A3. Physical vapor deposition processes; B1. Oxides; B2. Semiconducting II–VI materials

1. Introduction

The optical properties of ZnO have received increasing attention recently due to the promising applications of this material in short wavelength

optoelectronic devices as well as low voltage phosphors in flat panel display [1,2]. ZnO is an oxide semiconductor with band gap (3.3 eV) similar to GaN; the exciton binding energy of ZnO (60 meV) is much larger than that of GaN (25 meV), which enables efficient excitonic emission at room temperature [2]. Room temperature optical pumped lasing of ZnO has been observed in heteroepitaxial films, polycrystalline films,

*Corresponding author. Tel.: +65-67906439; fax: +65-67933318.

E-mail address: esplau@ntu.edu.sg (S.P. Lau).

multilayer quantum wells and nanowires [3–6]. The optoelectronic properties of material are sensitive to its crystal perfection. The photon emission efficiency decreases rapidly with the increase of non-radiative recombination centers. The crystal quality of ZnO films is determined not only by the growth processes, but also by the post-growth treatment, for example thermal annealing. Compared to the vast investigations on the effects of annealing on the luminescent properties of GaN and related materials [7–9], very little attention is paid to the annealing behaviors of luminescent properties of ZnO, and only a few works have been carried out [10–15]. Photoluminescence (PL) spectroscopy is a powerful tool in characterizing optical quality of semiconductor materials, such as PL intensity correlates directly with the defect densities in material. In general, PL spectrum of ZnO consists of two bands, near band edge (NBE) excitonic UV emission and defect related deep level emission (DLE) in the visible range. The two carrier recombination routes compete with each other during the luminescence process. The improvement of NBE by post-growth annealing has been reported. However, the annealing conditions were different for the different researchers, and ranges from ambient gas species, annealing temperature and annealing time [10–15]. Vanheusden et al. observed enhancement of NBE by annealing ZnO powders in a forming gas ($N_2:H_2$; 95:5 by volume) at 900°C , but at the same time, the intensity of DLE also increased considerably [10]. Shi et al. studied the annealing of ZnO films prepared by RF magnetron sputtering, and found that the improvement of NBE was only observed when hydrogen diluted argon was used as an ambient gas [11]. Ogata et al. reported that annealing in oxygen could improve the NBE of ZnO films prepared by molecular beam epitaxy [12]. Ozaki et al. and Cho et al. showed that both NBE and DLE were enhanced by annealing in air and nitrogen [13,14]. Low temperature hydrogen plasma doping method was proposed by Ohashi et al. who found that the NBE can be improved greatly through passivation of deep donors and acceptors with hydrogen [15]. The DLE recombination centers in ZnO degrade the emission efficiency of NBE. In order to obtain high

efficiency NBE, the formation of DLE during the annealing process should be suppressed. In this work, a face-to-face annealing approach is used which is commonly employed for III–V compound semiconductors [9]. The experimental results show that ZnO films annealed in face-to-face can enhance NBE but suppressed the DLE centers, as compared to samples annealed in open space.

2. Experiments

ZnO films used in the present studies were grown by filtered cathodic vacuum arc (FCVA) method. Details of the FCVA system have been described elsewhere [16]. Metallic zinc (purity 99.99%) was used as cathode target, and oxygen (purity 99.99%) was employed as the reactive gas. Films were deposited on quartz glass substrate. Growth parameters were optimized as follows: oxygen gas flow rate 50 sccm, chamber pressure 8×10^{-5} Torr, arc current 60 A, filter magnetic field 40 mT, and substrate temperature 250°C . The film thickness was measured by surface profiler to be around 200 nm for 5 min of deposition. The annealing was carried out in a standard Lindberg-type furnace using a quartz tube reactor at various temperatures. Samples were pushed into the hot zone of the quartz tube when the required temperature was reached. After annealing, samples were pulled out quickly and its temperature decreased to room temperature within 1 min. Face-to-face annealing of samples was carried out as shown in Fig. 1, where two ZnO films on quartz substrate were placed together, film surface to film surface, during annealing. This

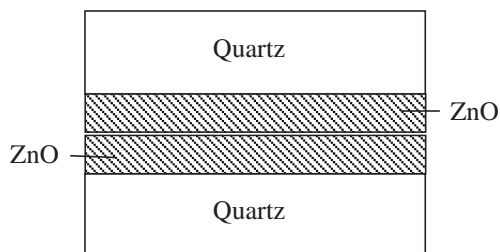


Fig. 1. Schematic structure used for face-to-face annealing, where two ZnO samples on quartz are placed together face to face during annealing.

arrangement confined the surface of the films that was exposed to the ambient during annealing. Three series of samples were prepared, (a) annealing in open air at temperatures ranging from 700°C to 900°C for 2 h, (b) annealing in open air at 900°C for different times, and (c) annealing in face-to-face at 900°C for different times. PL measurements were performed at room temperature and excited by the 325 nm line of a He–Cd laser with a power of 13 mW. Film surface morphology was characterized using field emission scanning electron microscopy (FESEM) (JEOL-6340F) and atomic force microscopy (AFM) (Nanoscope IIIa SPM, Digital Instruments, Inc).

3. Results and discussions

Fig. 2 shows a typical X-ray diffraction (XRD) pattern ($\theta/2\theta$ scan) of the as-grown ZnO films. The strong (002) peak at around 34.4° characterizes the hexagonal wurtzite structure of ZnO film with its *c*-axis normal to the substrate basal plane. The FWHM of the (002) peak is as small as 0.19°, which indicates the high crystal quality of the films. The films are dense and contain no droplet as observed by SEM. AFM measurements were performed in air. Fig. 3 shows an image scanned over areas of $2 \times 2 \mu\text{m}^2$. The film consists of grains with an average size of about 40 nm and rms roughness of 1.5 nm.

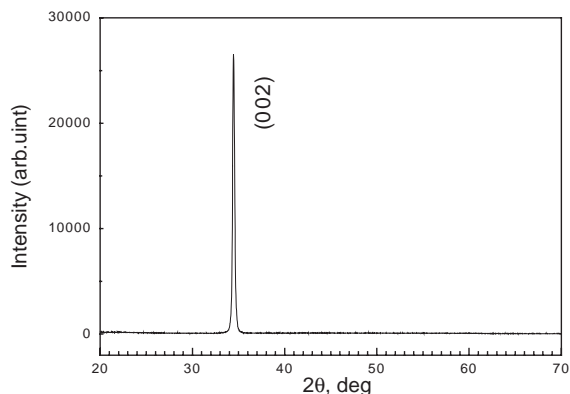


Fig. 2. $\theta/2\theta$ XRD pattern of as-grown ZnO film used for annealing.

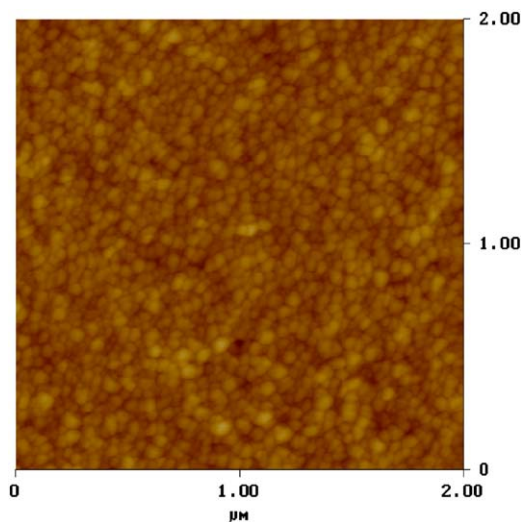


Fig. 3. AFM micrograph of as-grown ZnO film.

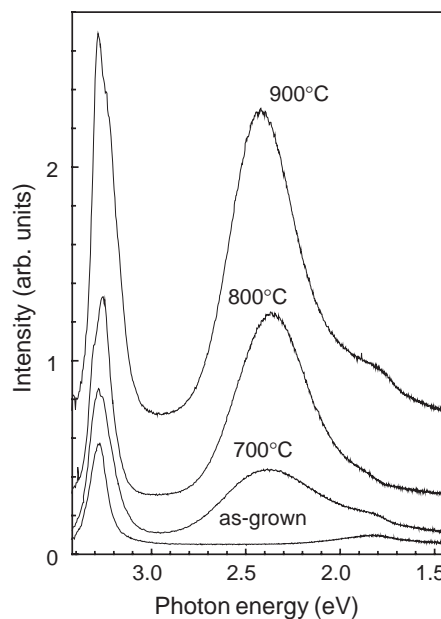


Fig. 4. PL spectra of as-grown film and films annealed in open air for 2 h at different temperatures.

Fig. 4 shows the PL spectra of the as-grown ZnO film and films annealed in open air for 2 h at 700°C, 800°C, and 900°C. For the as-grown film, an ultraviolet peak appears at 3.29 eV and its position is consistent with the reported room

temperature free exciton related NBE peak in ZnO films [3]. The intensity of DLE is much smaller than that of NBE. The DLE of the as-grown film is a broad peak centered at around 1.85 eV and it is similar to the oxygen interstitial related emission as suggested by Studenikin et al. [17]. The often-observed green emission band is not detected. Enhancement of NBE is clearly observed after thermal annealing in open air. The intensity of NBE increases with annealing temperature. However, the intensity of DLE also increases after annealing. The DLE is located in the visible spectrum and it consists of two bands. One weak band is located in the orange emission (1.85 eV), and the other one is located in the energy range similar to the green band at around 2.3–2.5 eV. The intensity of the green band increases significantly with annealing time, while the orange band only shows weak enhancement. These two luminescent bands have been reported previously [10,17]. However, the actual recombination mechanisms for these bands are still not fully understood. Oxygen vacancy, oxygen interstitial, zinc vacancy, and impurity are considered to be possible origins for these bands [10,18–22]. In this work, all the DLEs are found to be composed of two emission bands, however their positions and relative intensities vary with the annealing temperatures and times. The aim of this work is focused on the enhancement of NBE and the suppression of the DLE. In order to simplify the discussion, we will only consider the intensity of DLE as radiative recombination centers, and will not involve the mechanisms.

For annealing carried out in open air, the evolutions of the PL spectra with treatment time were studied systematically from 700°C to 900°C. The variations of PL spectra display similar time dependent trend for the different temperatures. The intensity of NBE increases initially with time, and with prolonged annealing, it decreases until the peak is undetectable. On the other hand, the intensity of DLE increases monotonically with annealing time. The DLE is dominated by the green emission band; and the relative intensity of the orange band becomes smaller with time, which indicates that the defect centers responsible for the orange band can be produced during the annealing

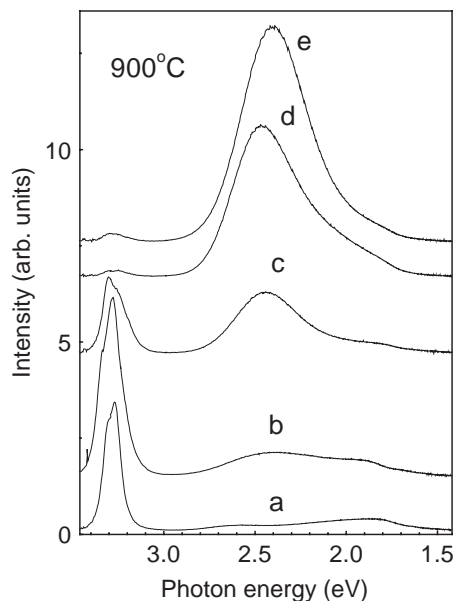


Fig. 5. The variation of PL spectra with annealing time at 900°C in open air. Curves (a)–(e) are acquired from films annealed for 1, 1.5, 2, 3 and 4 h, respectively.

process. The strongest NBE is recorded at an annealing temperature of 900°C. Fig. 5 shows the PL spectra from the samples annealed at 900°C for various times. For the films annealed for 1–2 h, the intensity of the NBE increases rapidly, and the DLE remains very weak though its intensity also increases together with the NBE. After 2 h of annealing, the intensity of DLE increases rapidly and that of NBE begins to degrade. This trend continues with further increase in annealing time, and finally the NBE becomes very weak and the DLE dominates the PL spectra as shown in curves (d) and (e) in Fig. 5, which corresponds to samples annealed for 3 and 4 h, respectively. The DLE is still dominated by the green emission band, and its position shifts to lower energy with annealing time.

The photon-excited non-equilibrium carriers in semiconductor recombine mainly via two routes—radiative and non-radiative recombination. For ZnO, the radiative recombination can be further separated into NBE and DLE as mentioned above. To improve the luminescent efficiency (NBE and DLE), the density of non-radiative recombination

centers in materials should be as low as possible. The non-radiative recombination centers can originate from many different sources, such as dislocations, point defects and surface/interface states. Threading dislocations are often considered to be the main non-radiative recombination centers in III–V arsenides, ZnSe-based II–VI and GaN based III–V semiconductors [23–25]. Recently, Karpov et al. estimated the influence of dislocation density on light emission efficiency, and found that emission efficiency can be close to unity when the dislocation density is reduced to about 10^7 cm^{-2} [26]. For ZnO, Ko et al. studied the PL properties of ZnO epilayers and suggested that threading dislocations played a key role on non-radiative recombination [27]. Non-radiative processes in bulk and epitaxial ZnO are found to be governed by zinc vacancy related complex and not by point defects from PL and positron annihilation analysis [28]. Non-radiative recombination centers are also attributed to surface or interface states at surface and grain boundaries, and their density is much higher in film with smaller grain size [29]. All these non-radiative recombination centers should coexist in any samples, but their relative contributions vary depending on the film growth conditions. The results shown in Figs. 4 and 5 manifest that the non-radiative recombination centers in our films can be annihilated effectively by post-growth annealing at high temperature. The removal of non-radiative recombination centers by annealing is a slow process and it may take hours for an annealing temperature of 900°C . The intensity of NBE reaches a maximum value after 1.5 h.

The monotonic increase of DLE with annealing time suggests that the DLE related defects cannot be removed by annealing, and on the contrary, the annealing conditions actually favor their formation. The massive increase in DLE intensity enables us to exclude the contribution of impurities to the DLE. If the DLE is from impurities, its intensity should depend largely on the concentration of impurities in the film. During the annealing process, it is more favorable to generate vacancy than interstitial defects, if an energy and chemical balance between the film and the ambient gas is considered. Oxygen and zinc vacancy can be

formed simultaneously and should be the most probable candidates for green emission band. However, whether it is oxygen or zinc vacancy or both vacancies which cause the DLE is still a matter of controversy [21,22,30]. It is interesting to note that the formation energies and diffusion behaviors of these two types of vacancies are very similar [21,22,31,32], so we will term them as vacancies. The low DLE intensities in as-grown film (Fig. 4) and curves (a) and (b) of Fig. 5 indicate that the concentrations of vacancies responsible for the DLE are insignificant in the as-grown films and in films annealed for a short time. In ZnO, the atomic displacement energies are 18.5 eV for zinc and 41.4 eV for oxygen according to the thermodynamic calculation by Van Vechten [33]. The high-energy electron irradiation experiment conducted by Look et al. showed that near-neighbor vacancy/interstitial Frenkel pairs were not stable in ZnO crystal lattice, and only defects with chain character could survive [34]. These facts indicate that the formation of vacancies within a perfect ZnO crystal is difficult. From PL spectra, it can be seen that the intensity of DLE and hence, its corresponding defects increase with annealing time. Vacancies can be formed easily at surface region. The vacancies in the bulk of ZnO can only come from the surface layer through diffusion. The hopping of an atom to a neighboring vacancy requires much less energy than the formation energy of a vacancy in a perfect lattice. The vacancy assisted diffusion of oxygen and zinc in ZnO have been investigated experimentally by Tomins et al. on single crystal ZnO [31,32]. The activation energies are found to be 3.85 eV for zinc and between 3.6 and 4.2 eV for oxygen. The imperfections in ZnO films, mainly grain boundaries, can facilitate the diffusion of oxygen or zinc in polycrystalline ZnO films, and in turn increase the rate of formation of vacancies. For polycrystalline films with small grain size, the vacancies formed through diffusion along grain boundaries could surpass that through top surface [35]. If the formation rate of vacancies surrounding the film surface can be controlled, then the density of DLE related defects in the bulk will be decreased, and ZnO films with higher NBE efficiency can be obtained.

The formation rate of vacancies at the surface region and the final equilibrium concentration of vacancies in ZnO are sensitive to the partial pressures of zinc and oxygen gas in the ambient [35]. High partial pressure can suppress the evaporation of zinc and oxygen atoms from the film surface and the formation of related vacancies at the surface region, and hence, the concentrations of vacancies in ZnO can be suppressed. Confining the space of the film surface that is exposed to the ambient is an effective method to increase the partial pressure surrounding the film surface. Here, we propose a simple method that can confine the space of the film exposed to the ambient where two ZnO samples are piled up such that the surface of each film face each other as shown in Fig. 1. Samples are annealed by this method at 900°C for various times, the respective PL spectra were obtained and shown in Fig. 6. Both the intensities of NBE and DLE bands increase with annealing time. This trend is similar to the samples that were annealed in open air. However, the most striking result is that the intensity of DLE is much smaller compared to films that were annealed in the open air for the same period of time. The ultraviolet NBE peak is

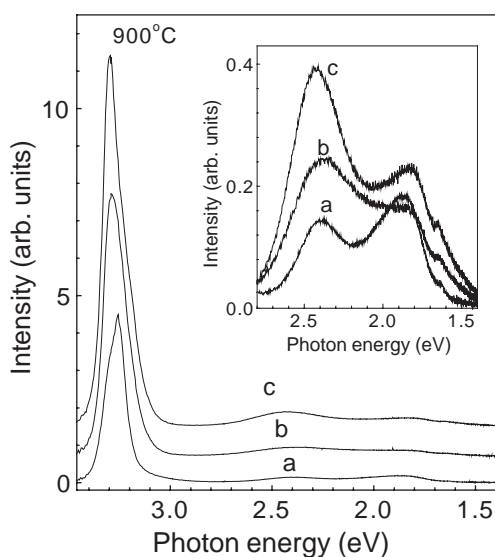


Fig. 6. PL spectra of films annealed at 900°C using face-to-face method for different times. Curves (a)–(c) correspond to annealing time of 1, 2 and 3 h, respectively.

enhanced significantly. The relative integrated intensities of NBE peaks for the as-grown film, film annealed in the open air at 900°C for 1.5 h and film annealed in face-to-face at 900°C for 3 h are 0.05, 0.6, and 1.3, respectively. The NBE is enhanced by a factor of about 12 and 26 times as compared to the as-grown film. By the face-to-face annealing method, the intensity of NBE increases with annealing time up to 3 h. This suggests that the annihilation of non-radiative defects in ZnO is a slow and time-consuming process. For films that were annealed in open air (Fig. 5), the improvement of NBE is only up to an annealing time of 1.5 h. For longer annealing time, the NBE is degraded due to the competition from the radiative recombination of DLE. As shown in the inset of Fig. 6, the DLEs of the films annealed in the face-to-face also composed of two main bands, which are similar to that observed in the films that were annealed in open air. The intensity of the green band increases slightly with annealing time. A weak peak around 1.65 eV is also observed. This is due to the second-order diffraction of the NBE, which is detectable only in the spectrum with intense NBE. It should be noted that similar NBE enhancement is observed if the samples are annealed in face-to-face, and it does not matter whether the second sample is a ZnO coated sample or a virgin quartz substrate.

The surface morphologies of ZnO films after annealing were characterized using SEM and AFM. The grain size in the films generally increases with increasing annealing temperature and time. It is found that surface roughness of the films annealed by the face-to-face method is much smaller than that annealed in open air. For comparison, Fig. 7(a) and (b) show two typical SEM images of the films annealed at 900°C for 2 h in open air and in face-to-face, respectively. For the film annealed in open air, grain sizes vary over a wide range from several tens nm to 200 nm, which is much larger than that of as-grown films (about 40 nm). The grains show well-defined crystal facet, and most grains orient with their (001) faces parallel to the substrate surface. The grains are loosely in contact with each other, lateral facets are exposed out and deep slits exist between grains. These suggest that for films annealed in open air,

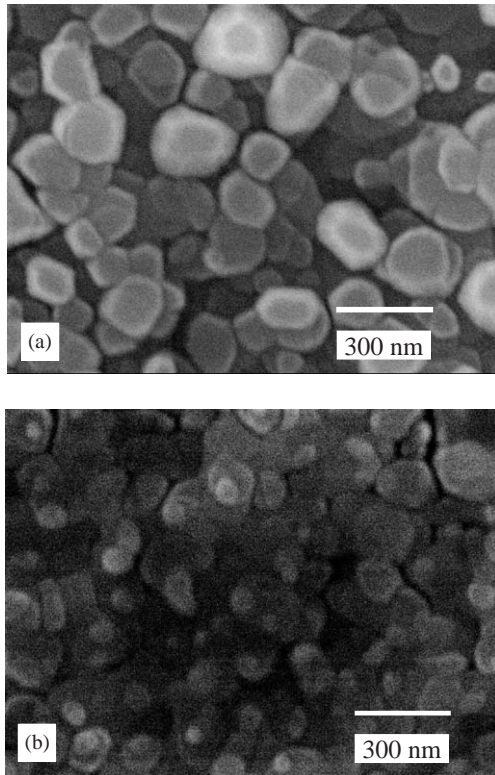


Fig. 7. SEM images of ZnO films after annealing at 900°C for 2 h for samples annealed in (a) open air, and (b) face-to-face.

strong coalescence and sublimation of ZnO grains take place. The surface morphology of the films annealed in the face-to-face is different. The grains are coalesced together intimately, grain boundaries cannot be distinguished clearly, and no well-defined crystal facets can be observed. These indicate that the face-to-face method has obviously prohibited or slowed down the sublimation rate of ZnO films during high temperature annealing. The rms roughness of the two films was measured by AFM. Its values increase from 1.5 nm for the as-grown film to around 30 and 10 nm for the films shown in Fig. 7(a) and (b), respectively. This is another advantage of the face-to-face annealing method, as smooth morphology is always required for most optoelectronic applications.

From the above analysis, the improvement of NBE efficiency by high temperature annealing originates from the reduction of non-radiative recombination centers in the films, and DLE

is enhanced in the same manner. This process is different from the hydrogen plasma doping method as suggested by Ohashi et al. [15], where the enhancement of ultraviolet emission of the latter is due to passivation of deep donors and acceptors via electron transfer between defects/impurity and hydrogen. Hydrogen forms n-type conduction in ZnO, and according to Karpov et al. n-type doping is more favorable for getting higher photon emission efficiency via saturation of the non-radiative recombination channel [26]. Recent investigations on the properties of hydrogen in ZnO showed that hydrogen is not thermally stable in ZnO [36]. Annealing at 500–600°C for 5 min is sufficient to release most of the hydrogen out of ZnO. So, if heating the samples to temperature higher than 500°C, the luminescent efficiency of hydrogen treated samples is expected to restore to its original value. The films annealed at high temperature show high thermal stability. Heating at temperatures up to 500°C in air has little effects on their luminescent properties. Another difference is that the non-radiative defect centers are removed from the films after high temperature annealing, while for hydrogen doping method, these defect centers still exist in the films and they are just temporary passivated. The degree of improvement of NBE is sample dependent. Our method can work well for ZnO, as non-radiative defect centers is the main factor that causes poor NBE emission efficiency. If DLE related defects is the main factor instead of non-radiative defect centers, this method will not work, and hydrogen doping method should be more suitable for such a case. In fact, ZnO films, prepared by various deposition techniques, always possess high density of non-radiative recombination centers that act as a main source of photon-excited free carrier recombination [28]. Thus, the face-to-face annealing method described here has its practical applications in enhancing ultraviolet NBE luminescent properties of ZnO films.

4. Conclusion

The dependence of luminescent properties of ZnO films on annealing conditions was investigated. The

ZnO films are highly (001) oriented. The NBE emission can be improved by annealing at high temperature through reduction of non-radiative recombination centers in the films. By face-to-face annealing, the luminescent efficiency of NBE ultraviolet emission is enhanced significantly while the formation of visible luminescence related defect centers is suppressed. This is attributed to the reduction of vacancies at the surface region and the low sublimation rate of ZnO films by face-to-face annealing. This method is applicable to films that have non-radiative recombination defect centers acting as the main carrier recombination route.

Acknowledgements

This work is supported by Agency for Science, Technology and Research (A*STAR) of Singapore.

References

- [1] C.G. Van de Walle, *Physica B* 308–310 (2001) 899.
- [2] D.C. Look, *Mater. Sci. Eng. B* 75 (2000) 190.
- [3] D.M. Bagnall, Y.F. Chen, Z. Zhu, T. Yao, S. Koyama, M.Y. Shen, T. Goto, *Appl. Phys. Lett.* 70 (1997) 2230.
- [4] A. Ohtomo, K. Tamura, M. Kawasaki, T. Makino, Y. Segawa, Z.K. Tang, G.K.L. Wong, Y. Matsumoto, K. Koinuma, *Appl. Phys. Lett.* 77 (2000) 2204.
- [5] S. Cho, J. Ma, Y. Kim, Y. Sun, G.K.L. Wong, J.B. Ketterson, *Appl. Phys. Lett.* 75 (1999) 2761.
- [6] M.H. Huang, S. Mao, H. Feick, H. Yan, Y. Wu, H. Kind, E. Weber, R. Russo, P. Yang, *Science* 292 (2001) 1897.
- [7] J.C. Zolper, M.H. Crawford, A.J. Howard, J. Ramer, S.D. Hersee, *Appl. Phys. Lett.* 68 (1996) 200.
- [8] A. Bell, I. Harrison, D. Korakakis, E.C. Larkins, J.M. Hayes, M. Kuball, N. Grandjean, J. Massies, *J. Appl. Phys.* 89 (2001) 1070.
- [9] H. Kanber, R.J. Cipolli, W.B. Henderson, J.M. Whelan, *J. Appl. Phys.* 57 (1984) 4732.
- [10] K. Vanhensden, W.L. Warren, C.H. Seager, D.R. Tallant, J.A. Voigt, B.E. Gnade, *J. Appl. Phys.* 79 (1996) 7983.
- [11] W.S. Shi, O. Agyeman, C.N. Xu, *J. Appl. Phys.* 91 (2002) 5640.
- [12] K. Ogata, K. Sakurai, S. Fujita, S. Fujita, K. Matsushige, *J. Crystal Growth* 214/215 (2000) 312.
- [13] J. Cho, J. Nah, M.S. Oh, J.H. Song, K.H. Yoon, H.J. Jung, W.K. Choi, *Jpn. J. Appl. Phys.* 40 (2001) L1040.
- [14] K. Ozaki, M. Gomi, *Jpn. J. Appl. Phys.* 41 (2002) 5614.
- [15] N. Ohashi, T. Ishigaki, N. Okada, T. Sekiguchi, I. Sakaguchi, H. Haneda, *Appl. Phys. Lett.* 80 (2002) 2869.
- [16] X.L. Xu, S.P. Lau, J.S. Chen, G.Y. Chen, B.K. Tay, *J. Crystal Growth* 233 (2001) 201.
- [17] S.A. Studenikin, N. Golego, M. Cocivera, *J. Appl. Phys.* 84 (1998) 2287.
- [18] D.C. Reynolds, D.C. Look, B. Jogai, *J. Appl. Phys.* 89 (2001) 6189.
- [19] X.L. Wu, G.G. Siu, C.L. Fu, H.C. Ong, *Appl. Phys. Lett.* 78 (2001) 2285.
- [20] N.Y. Garces, L. Wang, L. Bai, N.C. Giles, L.E. Halliburton, G. Cantwell, *Appl. Phys. Lett.* 81 (2002) 622.
- [21] A.F. Kohan, G. Ceder, D. Morgan, C.G. Van de Walle, *Phys. Rev. B* 61 (2000) 15019.
- [22] S.B. Zhang, S.-H. Wei, A. Zunger, *Phys. Rev. B* 63 (2001) 75205.
- [23] T. Hino, S. Tomiya, T. Miyajima, K. Yanashima, S. Hashimoto, M. Ikeda, *Appl. Phys. Lett.* 76 (2000) 3421.
- [24] S. Toyami, E. Morrita, M. Ukita, H. Okuyama, S. Itoh, K. Nakano, A. Ishibashi, *Appl. Phys. Lett.* 66 (1995) 1208.
- [25] J. Elsner, R. Jones, P.K. Sitch, V.D. Porezag, M. Elstner, Th. Frauenheim, M.I. Heggie, S. Oberg, P.R. Briddon, *Phys. Rev. Lett.* 79 (1997) 3672.
- [26] S.Y. Karpov, Y.N. Makarov, *Appl. Phys. Lett.* 81 (2002) 4721.
- [27] H.J. Ko, T. Yao, Y.F. Chen, S.K. Hong, *J. Appl. Phys.* 92 (2002) 354.
- [28] T. Koida, S.F. Chichibu, A. Uedono, A. Tsukazaki, M. Kawasaki, T. Sota, Y. Segawa, H. Koinuma, *Appl. Phys. Lett.* 82 (2003) 532.
- [29] T. Matsumoto, H. Kato, K. Miyamoto, M. Sano, E.A. Zhukov, T. Yao, *Appl. Phys. Lett.* 81 (2002) 1231.
- [30] S.A. Studenikin, M. Cocivera, *J. Appl. Phys.* 91 (2002) 5060.
- [31] G.W. Tomlines, J.L. Roubort, T.O. Mason, *J. Am. Ceram. Soc.* 81 (1998) 869.
- [32] G.W. Tomlines, J.L. Roubort, T.O. Mason, *J. Appl. Phys.* 87 (2000) 117.
- [33] J.A. Van Vechten, in: T.S. Moss, S.P. Keller (Eds.), *Handbook on Semiconductors*, North-Holland, Amsterdam, 1980 (Chapter. 1).
- [34] D.C. Look, J.W. Hemsky, J.R. Sizelove, *Phys. Rev. Lett.* 82 (1999) 2552.
- [35] H. Geistlinger, *J. Appl. Phys.* 80 (1996) 1370.
- [36] K. Ip, M.E. Overberg, Y.W. Heo, D.P. Norton, S.J. Pearton, C.E. Stutz, B. Luo, F. Ren, D.C. Look, J.M. Zavada, *Appl. Phys. Lett.* 82 (2003) 385.